Double DVCS (... and 2γ exclusive production)
- prospect for measurements

Jakub Wagner

National Centre for Nuclear Research, Warsaw

RBRC Workshop on Generalized Parton Distributions for Nucleon Tomography in the EIC Era

BNL, Jan 17 - 19, 2024

NATIONAL CENTRE FOR NUCLEAR RESEARCH ŚWIERK

- DVCS
  - is a main source of info about GPDs
  - a lot of activity on theory, exp, pheno side
  - rich plans for JLAB and EIC
- Other processes proposed and measured
  - Timelike Compton Scattering
  - Light meson production
  - Heavy meson production

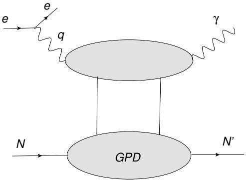

(a)

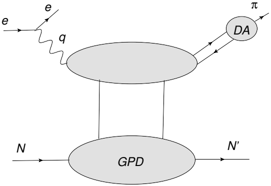

(c)

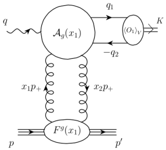

Figure 1: Kinematics of heavy vector meson photoproduction.

Limited and enhanced sensitivity

- All those processes (at least at LO) are sensitive only to $x = \xi$ line
- Non-invertability (Shadow GPDs and shedding light on them)

  $\longrightarrow$ P. Sznajder talk
- Another possible source of information about $x \neq \xi$ - lattice
- Other ideas: processes with more particles in the final states.

  $\longrightarrow$ Z.Yu talk
- Possible problems with factorization in the gluon exchange chanell reported recently:

  $\longrightarrow$ Nabeebaccus, Schönleber, Szymanowski, Wallon - 2311.09146

DDVCS

- Simplest:

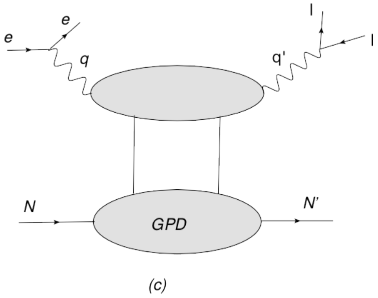

Double Deeply Virtual Compton Scattering (DDVCS): $\gamma N \to l^+ l^- N'$

- Proposed in:
  Belitsky & Muller, PRL 90, 022001 (2003)
  Guidal & Vanderhaeghen, PRL 90, 012001 (2003)
  Belitsky & Muller, PRD 68, 116005 (2003)
- No problems with factorization.

Berger, Diehl, Pire, 2002

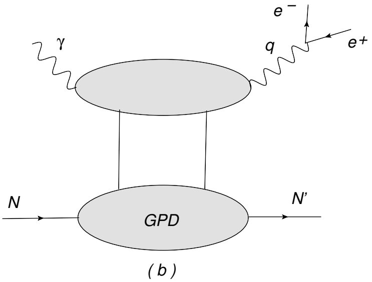

Timelike Compton Scattering (TCS): $\gamma N \to l^+ l^- N'$

Why TCS:

- universality of the GPDs
- another source for GPDs (special sensitivity on real part of GPD H)
- first step towards DDVCS
- spacelike-timelike crossing (different analytic structure - cut in Q^2)

D.Mueller, B.Pire, L.Szymanowski, J.Wagner, Phys.Rev.D86, 2012.

Thanks to simple spacelike-to-timelike relations, we can express the timelike CFFs by the spacelike ones in the following way:

$$
\begin{aligned}
{}^{T}\mathcal{H} &\overset{\mathrm{LO}}{=} {}^{S}\mathcal{H}^{*}\,, \\
{}^{T}\widetilde{\mathcal{H}} &\overset{\mathrm{LO}}{=} -{}^{S}\widetilde{\mathcal{H}}^{*}\,, \\
{}^{T}\mathcal{H} &\overset{\mathrm{NLO}}{=} {}^{S}\mathcal{H}^{*} - i\pi\,\mathcal{Q}^{2}\frac{\partial}{\partial\mathcal{Q}^{2}}\,{}^{S}\mathcal{H}^{*}\,, \\
{}^{T}\widetilde{\mathcal{H}} &\overset{\mathrm{NLO}}{=} -{}^{S}\widetilde{\mathcal{H}}^{*} + i\pi\,\mathcal{Q}^{2}\frac{\partial}{\partial\mathcal{Q}^{2}}\,{}^{S}\widetilde{\mathcal{H}}^{*}\,.
\end{aligned}
$$

The corresponding relations exist for (anti-)symmetric CFFs $\mathcal{E}$ ($\widetilde{\mathcal{E}}$).

DVCS vs TCS CFFs

O. Grocholski, H. Moutarde, B. Pire, P. Sznajder, J. Wagner, Eur.Phys.J. C80 (2020)

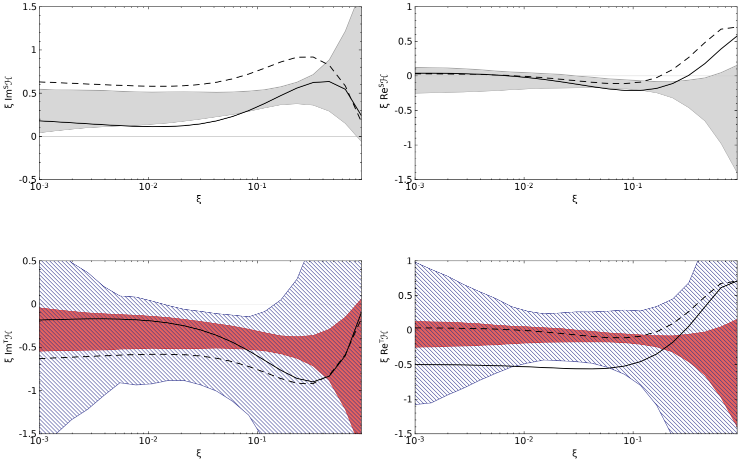

Imaginary (left) and real (right) part of DVCS (up) and TCS (down) CFF for $Q^2 = 2$ GeV^2 and $t = -0{,}3$ GeV^2 as a function of ξ. The shaded red (dashed blue) bands correspond to the data-driven predictions coming from the ANN global fit of DVCS data and they are evaluated using LO (NLO) spacelike-to-timelike relations. The dashed (solid) lines correspond to the GK GPD model evaluated with LO (NLO) coefficient functions.

The photon beam circular polarization asymmetry:

$$A_{CU} = \frac{\sigma^+ - \sigma^-}{\sigma^+ + \sigma^-} \sim Im(H)$$

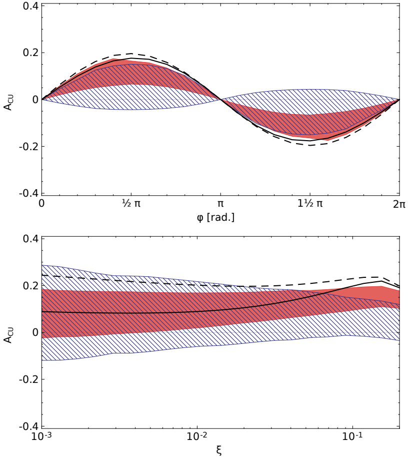

Circular asymmetry A_{CU} evaluated with LO and NLO spacelike-to-timelike relations for $Q'^2 = 4$ GeV^2, $t = -0{,}1$ GeV^2 and (left) $E_\gamma = 10$ GeV as a function of ϕ (right) and $\phi = \pi/2$ as a function of ξ. The cross sections used to evaluate the asymmetry are integrated over $\theta \in (\pi/4, 3\pi/4)$.

Experimental status

- First measurement: P. Chatagnon et al. (CLAS), PRL 127, 262501 (2021)

PHYSICAL REVIEW LETTERS **127,** 262501 (2021)

First Measurement of Timelike Compton Scattering

P. Chatagnon,[20,*] S. Niccolai,[20] S. Stepanyan,[36] M. J. Amaryan,[29] G. Angelini,[12] W. R. Armstrong,[1] H. Atac,[35] C. Ayerbe Gayoso,[44,†] N. A. Baltzell,[36] L. Barion,[13] M. Bashkanov,[42] M. Battaglieri,[36,15] I. Bedlinskiy,[25] F. Benmokhtar,[7] A. Bianconi,[39,19] L. Biondo,[15,18,40] A. S. Biselli,[8] M. Bondi,[15] F. Bossù,[3] S. Boiarinov,[36] W. J. Briscoe,[12] W. K. Brooks,[37,36]

- TCS has the same final state as J/ψ, already measured in UPCs! LHCb, CMS, ALICE, AFTER

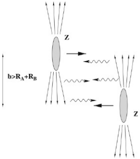

$$\sigma^{AB} = \int dk_A \frac{dn^A}{dk_A} \sigma^{\gamma B}(W_A(k_A)) + \int dk_B \frac{dn^B}{dk_B} \sigma^{\gamma A}(W_B(k_B))$$

- Measurement of TCS should also make us **more optimistic** about DDVCS!

Double DVCS

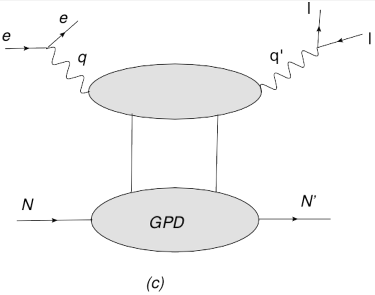

Double Deeply Virtual Compton Scattering (DDVCS): $\gamma N \to l^+ l^- N'$

$$\gamma^*(q_{in}) N(p) \to \gamma^*(q_{out}) N'(p')$$

Variables, describing the processes of interest in this generalized Bjorken limit, are the scaling variable ξ and skewness $\eta > 0$:

$$\xi = -\frac{q_{out}^2 + q_{in}^2}{q_{out}^2 - q_{in}^2}\eta\,, \quad \eta = \frac{q_{out}^2 - q_{in}^2}{(p+p')\cdot(q_{in}+q_{out})}\,.$$

- DDVCS: $q_{in}^2 < 0\,, \quad q_{out}^2 > 0\,, \quad \eta \neq \xi$
- DVCS: $q_{in}^2 < 0\,, \quad q_{out}^2 = 0\,, \quad \eta = \xi > 0$
- TCS: $q_{in}^2 = 0\,, \quad q_{out}^2 > 0\,, \quad \eta = -\xi > 0$

CFFs are the GPD dependent quantities which enter the amplitudes. They are defined through relations:

$$\mathcal{A}^{\mu\nu}(\xi,\eta,t) = -e^2 \frac{1}{(P+P')^+}\,\bar{u}(P')\left[g_T^{\mu\nu}\left(\mathcal{H}(\xi,\eta,t)\,\gamma^+ + \mathcal{E}(\xi,\eta,t)\,\frac{i\sigma^{+\rho}\Delta_\rho}{2M}\right)\right.$$
$$\left. + i\epsilon_T^{\mu\nu}\left(\widetilde{\mathcal{H}}(\xi,\eta,t)\,\gamma^+\gamma_5 + \widetilde{\mathcal{E}}(\xi,\eta,t)\,\frac{\Delta^+\gamma_5}{2M}\right)\right] u(P)\,,$$

,where:

$$\begin{aligned}
\mathcal{H}(\xi,\eta,t) &= +\int_{-1}^{1} dx \left(\sum_q T^q(x,\xi,\eta)H^q(x,\eta,t) + T^g(x,\xi,\eta)H^g(x,\eta,t)\right)\\
\widetilde{\mathcal{H}}(\xi,\eta,t) &= -\int_{-1}^{1} dx \left(\sum_q \widetilde{T}^q(x,\xi,\eta)\widetilde{H}^q(x,\eta,t) + \widetilde{T}^g(x,\xi,\eta)\widetilde{H}^g(x,\eta,t)\right).
\end{aligned}$$

- DVCS vs TCS

$$
\begin{aligned}
{}^{DVCS}T^q &= -e_q^2 \tfrac{1}{x+\eta-i\varepsilon} - (x \to -x) = & ({}^{TCS}T^q)^* \\
{}^{DVCS}\tilde{T}^q &= -e_q^2 \tfrac{1}{x+\eta-i\varepsilon} + (x \to -x) = & -({}^{TCS}\tilde{T}^q)^*
\end{aligned}
$$

$$
{}^{DVCS}Re(\mathcal{H}) \sim P \int \frac{1}{x \pm \eta} H^q(x,\eta,t)\,, \quad {}^{DVCS}Im(\mathcal{H}) \sim i\pi H^q(\pm\eta,\eta,t)
$$

- DDVCS

$$
{}^{DDVCS}T^q = -e_q^2 \frac{1}{x+\xi-i\varepsilon} - (x \to -x)
$$

$$
{}^{DDVCS}Re(\mathcal{H}) \sim P \int \frac{1}{x \pm \xi} H^q(x,\eta,t)\,, \quad {}^{DVCS}Im(\mathcal{H}) \sim i\pi H^q(\pm\xi,\eta,t)
$$

DDVCS can provide unique information, but is very challenging experimentally. But recent measurement of TCS should also make us more optimistic about DDVCS!

We need muon detection!

Deja, Martínez-Fernández, Pire, Sznajder, JW, **PRD 107 (2023)**

- In the view of new experiments, revisiting DDVCS is timely
- DDVCS is a subprocess in the electroproduction of a lepton pair

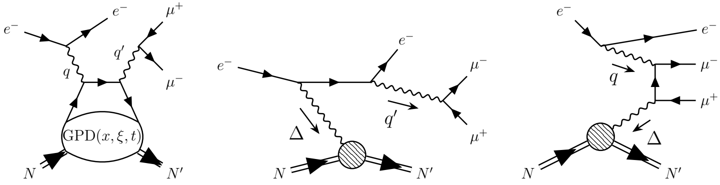

(from left to right) DDVCS, BH1, BH2.

- Rederivation of DDVCS formulae via Kleiss-Stirling's methods:
  - Direct calculation of amplitudes
  - 2 scalars as building blocks, a and b as light-like vectors:

$$s(a,b) = \bar{u}(a,+)u(b,-) = -s(b,a)$$
$$t(a,b) = \bar{u}(a,-)u(b,+) = [s(b,a)]^*$$
$$s(a,b) = (a^2 + ia^3)\sqrt{\frac{b^0 - b^1}{a^0 - a^1}} - (a \leftrightarrow b)$$

Kleiss & Stirling, Nuclear Physics B262 (1985) 235-262

- DDVCS subprocess amplitude:

$$i\mathcal{M}_{\mathrm{DDVCS}}=\frac{-ie^4}{(Q^2-i0)(Q'^2+i0)}\left(i\mathcal{M}^{(V)}_{\mathrm{DDVCS}}+i\mathcal{M}^{(A)}_{\mathrm{DDVCS}}\right)$$

- Vector contribution:

$$i\mathcal{M}^{(V)}_{\mathrm{DDVCS}}=-\frac{1}{2}\left[f(s_\ell,\ell_-,\ell_+;s,k',k)-g(s_\ell,\ell_-,n^\star,\ell_+)g(s,k',n,k)-g(s_\ell,\ell_-,n,\ell_+)g(s,k',n^\star,k)\right]$$
$$\times\left[(\mathcal{H}+\mathcal{E})[Y_{s_2s_1}g(+,r'_{s_2},n,r_{s_1})+Z_{s_2s_1}g(-,r'_{-s_2},n,r_{-s_1})]-\frac{\mathcal{E}}{M}\mathcal{J}^{(2)}_{s_2s_1}\right]$$

- Axial contribution:

$$i\mathcal{M}^{(A)}_{\mathrm{DDVCS}}=\frac{-i}{2}\epsilon^{\mu\nu}_{\perp}j_\mu(s_\ell,\ell_-,\ell_+)j_\nu(s,k',k)\left[\widetilde{\mathcal{H}}\mathcal{J}^{(1,5)+}_{s_2s_1}+\widetilde{\mathcal{E}}\frac{\Delta^+}{2M}\mathcal{J}^{(2,5)+}_{s_2s_1}\right]$$

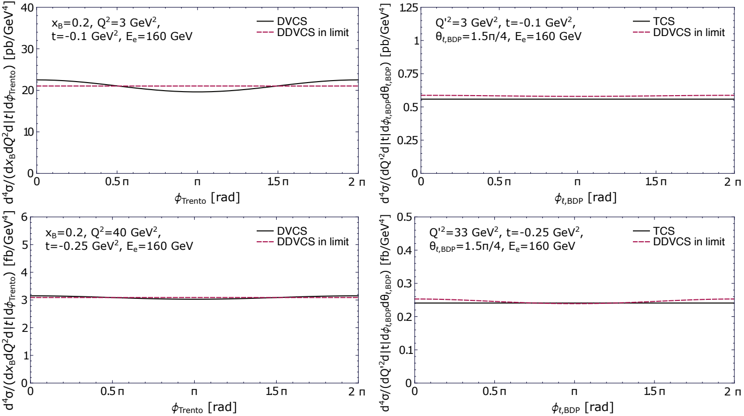

Comparison of DDVCS and (left) DVCS and (right) TCS cross-sections for pure VCS subprocess.

- We consider $Q'^2 > Q^2$: our DDVCS is "more" timelike than spacelike

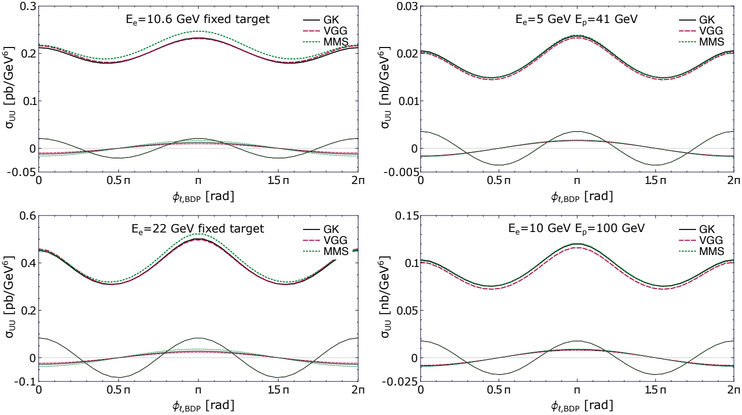

JLab12, JLab20+ EIC 5x41, EIC 10x100

Experiment	Beam energies [GeV]	y	$\lvert t\rvert$ [GeV^2]	Q^2 [GeV^2]	Q'^2 [GeV^2]
JLab12	$E_e = 10{,}6,\ E_p = M$	0,5	0,2	0,6	2,5
JLab20+	$E_e = 22,\ E_p = M$	0,3	0,2	0,6	2,5
EIC	$E_e = 5,\ E_p = 41$	0,15	0,1	0,6	2,5
EIC	$E_e = 10,\ E_p = 100$	0,15	0,1	0,6	2,5

Observables: beam-spin asymmetry

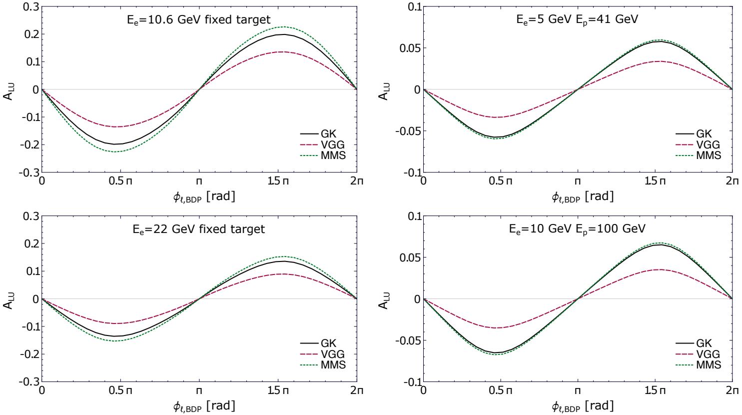

JLab12, JLab20+: up to **15-20 %** EIC 5x41, EIC 10x100: **3-7 %**

Experiment	Beam energies [GeV]	y	$\lvert t\rvert$ [GeV^2]	Q^2 [GeV^2]	Q'^2 [GeV^2]
JLab12	$E_e = 10{,}6,\ E_p = M$	0,5	0,2	0,6	2,5
JLab20+	$E_e = 22,\ E_p = M$	0,3	0,2	0,6	2,5
EIC	$E_e = 5,\ E_p = 41$	0,15	0,1	0,6	2,5
EIC	$E_e = 10,\ E_p = 100$	0,15	0,1	0,6	2,5

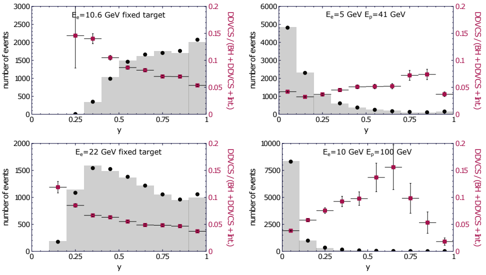

JLab12, JLab20+ EIC 5x41, EIC 10x100

EpIC MC
integrated cross-section
pure DDVCS fraction

Kinematic cuts:
$Q^2 \in (0{,}15,\, 5)$ GeV^2
$Q'^2 \in (2{,}25,\, 9)$ GeV^2
JLab: $-t \in (0{,}1,\, 0{,}8)$ GeV^2
EIC: $-t \in (0{,}01,\, 1)$ GeV^2
$\phi, \phi_\ell \in (0{,}1,\, 2\pi - 0{,}1)$ rad
$\theta_\ell \in (\pi/4,\, 3\pi/4)$ rad
JLab: $y \in (0{,}1,\, 1)$
EIC: $y \in (0{,}05,\, 1)$

10000 events/distribution. Neither acceptance nor detectors response are taken into account in this study

Experiment	Beam energies [GeV]	Range of $\lvert t\rvert$ [GeV^2]	$\sigma\vert_{0<y<1}$ [pb]	$\mathcal{L}^{10k}\vert_{0<y<1}$ [fb^{-1}]	$y_{\min}$	$\sigma\vert_{y_{\min}<y<1}/\sigma\vert_{0<y<1}$
JLab12	$E_e = 10{,}6,\ E_p = M$	$(0{,}1, 0{,}8)$	0,14	70	0,1	1
JLab20+	$E_e = 22,\ E_p = M$	$(0{,}1, 0{,}8)$	0,46	22	0,1	1
EIC	$E_e = 5,\ E_p = 41$	$(0{,}05, 1)$	3,9	2,6	0,05	0,73
EIC	$E_e = 10,\ E_p = 100$	$(0{,}05, 1)$	4,7	2,1	0,05	0,32

Summary DDVCS

- New analytical formulae for the electroproduction of a lepton pair have been derived.
- Asymmetries are large enough for DDVCS to be measurable at both current (JLab12) and future (JLab20+, EIC) experiments
- Implemented in PARTONS and EpIC MC (LO + LT)
- Higher Twist needed (also for DVCS and TCS) and we are working on it.

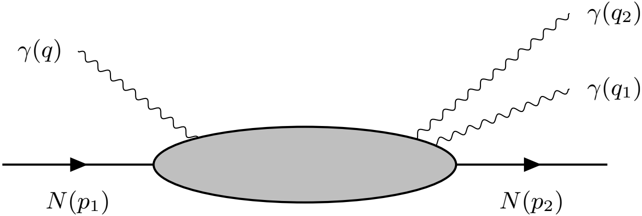

- Photo- and Electroproduction of photon pairs with large invariant mass:

$$\gamma\ N \rightarrow \gamma\ \gamma\ N$$

- The hard part is a $2 \rightarrow 3$ reaction, a new type of processes studied within the framework of QCD collinear factorization.
- The amplitude depends only on charge-odd combinations of GPDs (only valence quarks contribute):
  - **DVCS:** $\sum_q e_q^2 \left(H^q(x,\xi) - H^q(-x,\xi)\right)$ and $H^g(x)$
  - **Diphoton:** $\sum_q e_q^3 \left(H^q(x,\xi) + H^q(-x,\xi)\right)$ and no gluons
- No gluonic GPD contribution - cleaner and safer (factorization).

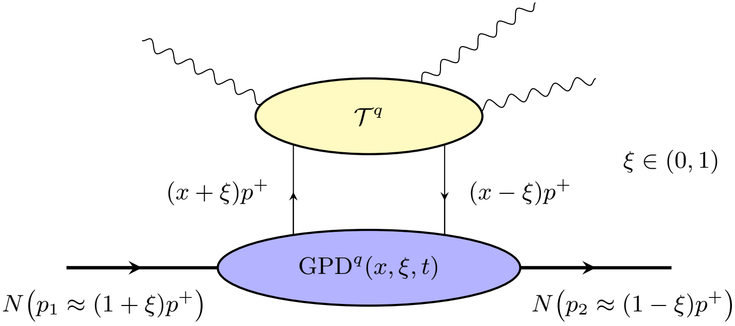

The full amplitude:

$$\mathcal{T} = \sum_q \int_{-1}^{1} dx\, \mathcal{T}^q\big(x,\xi,\ldots\big)\mathrm{GPD}^q(x,\xi,t).$$

A. Pedrak , B. Pire , L. Szymanowski , JW, Phys. Rev. D 96 (2017)

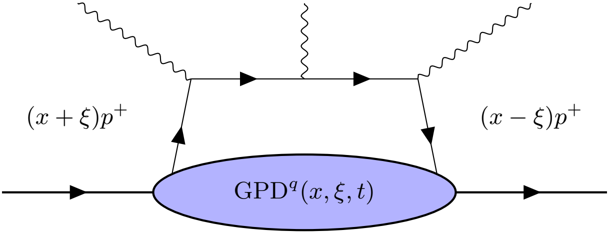

The process can be studied at intense quasi-real photon beam facilities in JLab or EIC.

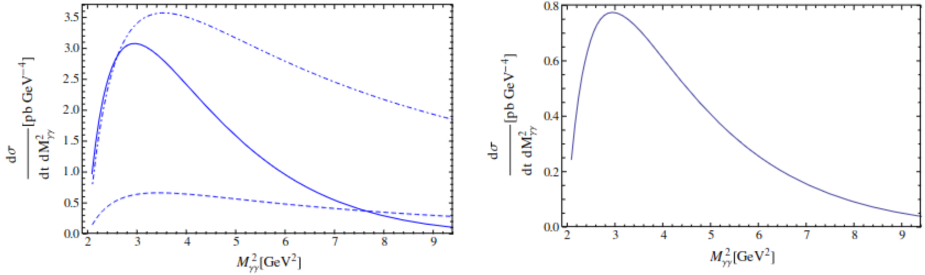

FIG. 5. The $M^2_{\gamma\gamma}$ dependence of the unpolarized differential cross section $\frac{d\sigma}{dM^2_{\gamma\gamma}dt}$ on a proton (left panel) and on a neutron (right panel) at $t = t_{\min}$ and $S_{\gamma N} = 20$ GeV^2 (full curves), $S_{\gamma N} = 100$ GeV^2 (dashed curve) and $S_{\gamma N} = 10^6$ GeV^2 (dash-dotted curve, multiplied by 10^5).

NLO factorization:
O. Grocholski , B. Pire , P. Sznajder , L. Szymanowski , JW, Phys. Rev. D 104 (2021) [2110.00048]

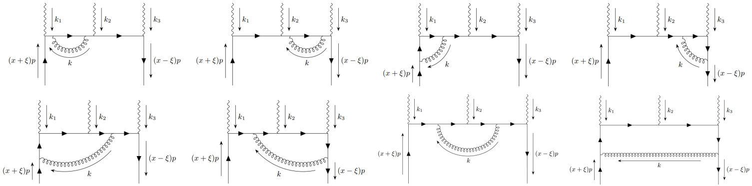

Considered 1-loop diagrams

Next-to-leading order results

- 2- and 3-point loops $\rightarrow$ relatively simple results.
- 5-point loop integral can be reduced to a sum 4-point ones.
- Finite part of a 4-point diagrams: expressible in terms of

$$\mathcal{F}_{nab} := \int_0^1 dy \int_0^1 dz\, y^a z^b \Big(\alpha_1 y + \alpha_2 z + \alpha_3 yz + i\epsilon\Big)^{-n},$$

$$\mathcal{G} := \int_0^1 dy \int_0^1 dz\, z^2 \Big(\alpha_1 y + \alpha_2 z + \alpha_3 yz + i\epsilon\Big)^{-2} \times \log\Big(\alpha_1 y + \alpha_2 z + \alpha_3 yz + i\epsilon\Big).$$

Large computational power is needed to get stable results.

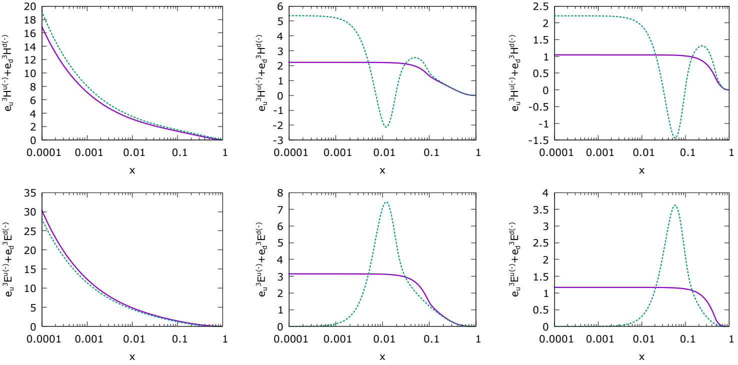

Comparison between GK [hep-ph/0708.3569] (solid magenta) and MMS [hep-ph/1304.7645] (dotted green) GPD models for $t = -0{,}1\ \mathrm{GeV}^2$ and the scale $\mu_F^2 = 4\ \mathrm{GeV}^2$ for $\xi = x$ $\xi = 0{,}1$ $\xi = 0{,}5$.

H^q, E^q - vector GPDs, $\tilde{H}^q, \tilde{E}^q$ - axial GPDs.

$$\mathcal{H} = \sum_q \int_{-1}^{1} dx \, \mathcal{T}^q(x, \xi, ...) H^q(x, \xi, t),$$

$\mathcal{E}, \tilde{\mathcal{H}}, \tilde{\mathcal{E}}$ defined in the analogous way.

Contribution from axial GPDs is small at LO, we neglect it in the NLO analysis.

Stability of results

O. Grocholski , B. Pire , P. Sznajder , L. Szymanowski , JW, Phys.Rev.D 105 (2022)

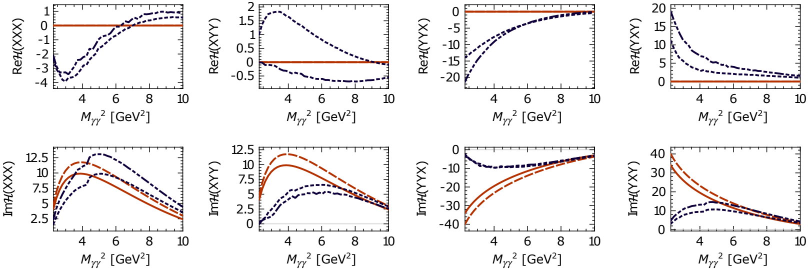

$\mathcal{H}$ as a function of $M_{\gamma\gamma}$ for $S_{\gamma N} = 20\ \mathrm{GeV}^2$, $t = t_0$ and $u' = -1\ \mathrm{GeV}^2$.

LO: solid (dashed) red line
NLO: dotted (dash-dotted) blue line
for GK (MMS) GPD model

Differential cross section: $S_{\gamma N}$-dependence

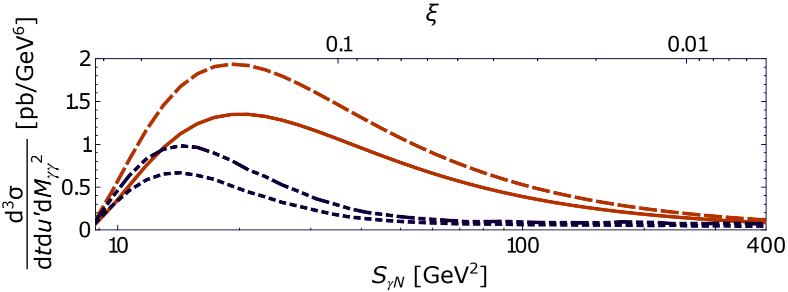

Differential cross-section as a function of $S_{\gamma N}$ (bottom axis) and the corresponding ξ (top axis) for $M^2_{\gamma\gamma} = 4\ \mathrm{GeV}^2$, $t = t_0$ and $u' = -1\ \mathrm{GeV}^2$.

LO: solid (dashed) red line
NLO: dotted (dash-dotted) blue line
for GK (MMS) GPD model

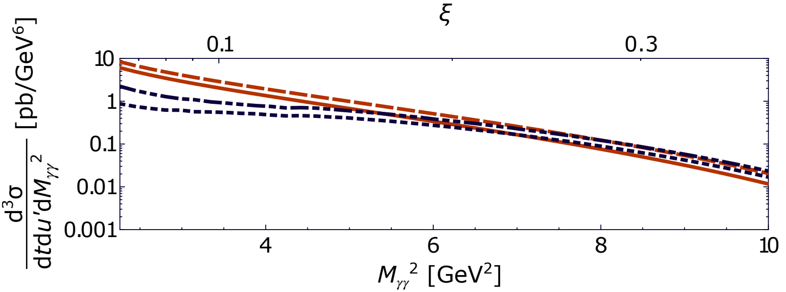

Differential cross-section as a function of $M_{\gamma\gamma}^2$ (bottom axis) and the corresponding ξ (top axis) for $S_{\gamma N} = 20\ \mathrm{GeV}^2$, $t = t_0$ and $u' = -1\ \mathrm{GeV}^2$.

LO: solid (dashed) red line
NLO: dotted (dash-dotted) blue line
for GK (MMS) GPD model

Exclusive diphoton photoproduction

B. Skura (Warsaw U. of Technology), PS
preliminary results

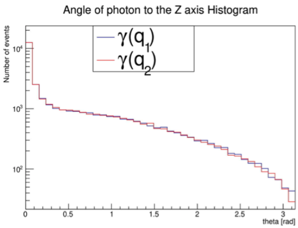

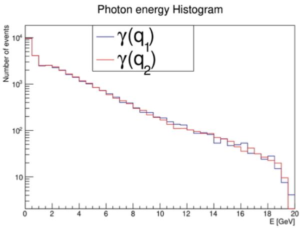

- The process implemented in EpIC MC generator with equivalent-photon approximation

$$\frac{\mathrm{d}^6\sigma}{\mathrm{d}Q^2\,\mathrm{d}y\,\mathrm{d}t\,\mathrm{d}u'\,\mathrm{d}M^2_{\gamma\gamma}\mathrm{d}\phi} = \Gamma(y, Q^2)\times\frac{\mathrm{d}^4\sigma_{2\gamma}}{\mathrm{d}t\,\mathrm{d}u'\,\mathrm{d}M^2_{\gamma\gamma}\mathrm{d}\phi}$$

- Condition used in generation of events

E = 20 GeV

$0 < -t < 1$ GeV^2
$0 < -u < 6$ GeV^2
1 GeV^2 $< M_{\gamma\gamma}^2 <$ 5 GeV^2
$0 < \phi < 2\pi$

$0 < y < 1$
$0 < Q^2 < 0.01$ GeV^2

- Event counts are scaled to 10 fb^{-1}

Electroproduction and Bethe-Heitler contributions

A. Pedrak , B. Pire , L. Szymanowski , JW, Phys.Rev.D 101 (2020)

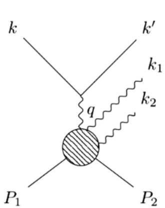

FIG. 1. The QCD process contributing to $eN \to e'\gamma\gamma N'$.

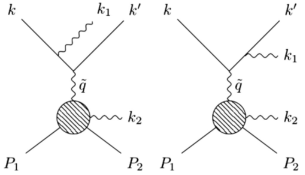

FIG. 2. The single Bethe-Heitler process contributing to $eN \to e'\gamma\gamma N'$. Two other graphs with $k_1 \leftrightarrow k_2$ interchange are not shown.

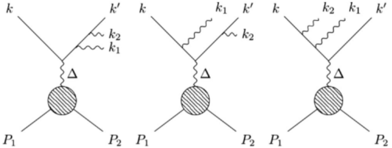

FIG. 3. The double Bethe-Heitler process contributing to $eN \to e'\gamma\gamma N'$. Three other graphs with $k_1 \leftrightarrow k_2$ interchange are not shown.

Access to $x \neq \xi$.

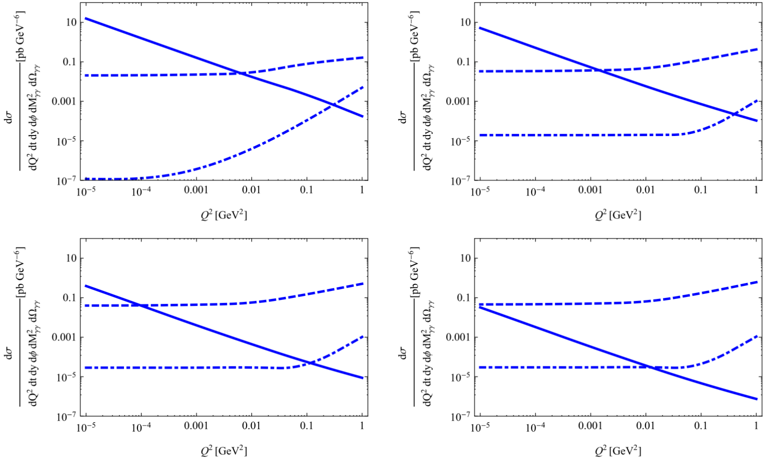

FIG. 10. The relative importance of the different processes contributing to $eN \to e'\gamma\gamma N'$—shown here (from left to right and from top to bottom) for $s = 20$ GeV^2, $s = 100$ GeV^2, $s = 1000$ GeV^2 and $s = 10000$ GeV^2 at the kinematical point $M^2_{\gamma\gamma} = 3$ GeV^2, $\theta_{\gamma\gamma} = 3\pi/8$, $\phi_{\gamma\gamma} = 0$, $y = 0.6$—depends much on the value of Q^2. The QCD process (solid curve) dominates at very low Q^2, the single Bethe-Heitler process (dashed curve) dominates at higher Q^2, while the double Bethe-Heitler process (dotted curve) is always subdominant.

2γ - Summary

- $\gamma N \to \gamma\gamma N$ can provide valuable information about charge-odd combinations of GPDs,
- We performed a next-to-leading order analysis of the diphoton photoproduction process,
- NLO corrections result in smaller cross sections,
- Electroproduction gives a chance to access $x \neq \xi$ line
- Implemented in PARTONs and EpIC MC